IOPscience iopscience.iop.org

Home Search Collections Journals About Contact us My IOPscience

# Magnetic anomalies near energy level crossing in $HoPO_4$

This article has been downloaded from IOPscience. Please scroll down to see the full text article.

2003 J. Phys.: Condens. Matter 15 8767

(http://iopscience.iop.org/0953-8984/15/50/010)

View the table of contents for this issue, or go to the journal homepage for more

Download details:
IP Address: 171.66.16.125
The article was downloaded on 19/05/2010 at 17:53

Please note that terms and conditions apply.

INSTITUTE OF PHYSICS PUBLISHING JOURNAL OF PHYSICS: CONDENSED MATTER

J. Phys.: Condens. Matter **15** (2003) 8767–8779 PII: S0953-8984(03)68194-4

# Magnetic anomalies near energy level crossing in $HoPO_4$

**J-M Broto[1], H Rakoto[1] and Z A Kazei[2,3]**

[1] LNCMP, avenue de Rangueil 143, 31432 Toulouse, Cedex 4, France
[2] Physics Department, Moscow State University, Vorob'evy Gory, 119899 Moscow, Russia

E-mail: kazei@plms.phys.msu.su

Received 31 August 2003, in final form 3 November 2003
Published 3 December 2003
Online at stacks.iop.org/JPhysCM/15/8767

**Abstract**

Anomalies of magnetic properties caused by the interaction of energy levels of the rare-earth ion in $HoPO_4$ in a high magnetic field along the [100] and [110] axes are investigated experimentally and theoretically. Jumps in the magnetization curves $M(H)$ and maxima in their derivatives $dM(H)/dH$ are observed at critical fields $H_c = 200$ and 320 kOe where one of excited singlets approaches or crosses the lowest energy level of the $Ho^{3+}$ ion. The experimental data are found to be described rather accurately by the calculated magnetic moments $M(H)$ along the [100] and [110] axes when taking into account the quadrupolar interactions and magnetocaloric effect at the adiabatic magnetization in pulsed fields. It is shown that a jump-like change of the quadrupolar interactions of $\alpha$ and $\gamma$ (or $\delta$) symmetry in $HoPO_4$ caused by a change in the corresponding quadrupolar moments upon level crossing leads, according to the experiment, to a decrease of the critical field $H_c$ and a sharper variation of the $M(H)$ and $dM(H)/dH$ curves near the crossover.

## 1. Introduction

Rare-earth (RE) paramagnets with the tetragonal zircon structure $RXO_4$ (X = P, As, and V; space group $D_{19}^{4h} = I4_1/amd$) are very convenient for the study of crystal field (CF) effects, such as crossing of the energy levels (crossover) of rare-earth ions in a magnetic field. The energy level crossing effects in high magnetic fields provide valuable information about the energy level scheme and wavefunctions of an RE ion formed by the CF couplings. An analysis shows that the crossover occurs for almost all RE vanadates and phosphates with the zircon structure in high and ultrahigh magnetic fields [1]. The crossover was observed and studied in detail for RE zircons $HoVO_4$ [2–4], $YbPO_4$ [5], $PrVO_4$ [6] and $TmPO_4$ [7] for a magnetic field along the tetragonal axis. In this case a true crossing of the lower levels without a gap takes

[3] Author to whom any correspondence should be addressed.

0953-8984/03/508767+13$30.00 © 2003 IOP Publishing Ltd Printed in the UK 

place, and is accompanied by sharp jumps in the magnetization curves at low temperatures. A magnetic field perpendicular to the tetragonal axis most often mixes the wavefunctions of the interacting levels (mixes the states that differ by the projections $\Delta J_z = \pm 1$), i.e., results in a repulsion of the levels and the occurrence of a finite gap near the crossover. This type of crossover was observed in $DyPO_4$ for a magnetic field along the [100] and [110] axes in the basal plane [8].

One can also note a new aspect of these studies. RE zircons are known to reveal numerous effects caused by quadrupolar interactions, for example spontaneous and magnetic field induced quadrupolar orderings (Jahn–Teller structural phase transitions) [9, 10]. Reliable experimental data on the interaction parameters of these compounds, in conjunction with modern theoretical approaches, allow not only the qualitative study of the quadrupolar effects but also their description on a good quantitative level. The profound change of the electron structure of RE ions (their spectra and wavefunctions) at the crossover is accompanied by a jump-like change both of the magnetic and various quadrupolar moments. A high magnetic field may form near the crossover low-lying electronic states with high quadrupolar moments, rendering large quadrupolar effects. Thus the crossover is expected to lead to a variation of the quadrupolar contributions to the magnetic properties, which depend on both quadrupolar constants and quadrupolar moments determined by the electron structure of an RE ion.

One of the promising candidates for further experimental studies of the crossover effects is $HoPO_4$. Holmium phosphate is known not to reveal noticeable quadrupolar effects without a magnetic field. The bilinear interactions are also not very large, and give rise to an antiferromagnetic ordering of the $Ho^{3+}$ magnetic moments along the $c$ axis at 1.4 K [11]. The CF mixing gives rise to highly anisotropic low-lying energy levels of the $Ho^{3+}$ ion, which are responsible for Ising-type behaviour. Measurements of the magnetic susceptibility, magnetic moment and specific heat of holmium phosphate give evidence for its high magnetic anisotropy [11–13]. In this work the magnetic anomalies near crossover in $HoPO_4$ are studied experimentally and theoretically in a high magnetic field, and the effects of the quadrupolar interactions are analysed.

## 2. Samples and measuring technique

Magnetization $M(H)$ and magnetic susceptibility $\mathrm{d}M(H)/\mathrm{d}H$ of a $HoPO_4$ crystal were studied in a field along the [100] and [110] axes in the temperature range 1.4–15 K. The well-known method of spontaneous crystallization from the solution in the melt was used to grow single crystals of $HoPO_4$ with a $PbO$–$PbF_2$–$PbP_2O_6$–$H_3BO_3$ melt as a solvent. The crystals were transparent and slightly coloured; their length was about 2–3 mm in each direction of the crystallographic cell. A sample crystal was oriented along the measured axis by an x-ray method with an accuracy $\pm 1°$–$2°$ and was mounted on a plastic rod. No additional alignment of the crystal along the magnetic field was allowed during the measurements so the total accuracy of the crystal alignment was estimated within $\pm 3°$. RE zircon crystals are layered and brittle, which hinders measurements of their magnetic properties in pulsed magnetic fields. To protect the sample against cracking during the high field measurements, it was inserted into a drop of epoxy.

The measurements were made by the induction method in pulsed magnetic fields up to 360 kOe. The rise and fall times of the magnetic field in the pulse were 100 and 700 ms, respectively. Digital recording of the signals from the measuring $M(t)$ and field $H(t)$ coils was made with a step of $\sim$0.5 kOe during the field pulse (about 800 points). The decompensation signal of the measuring coil was recorded under the same conditions in the absence of a sample and subtracted by a program. The programmed experimental data processing consisted of

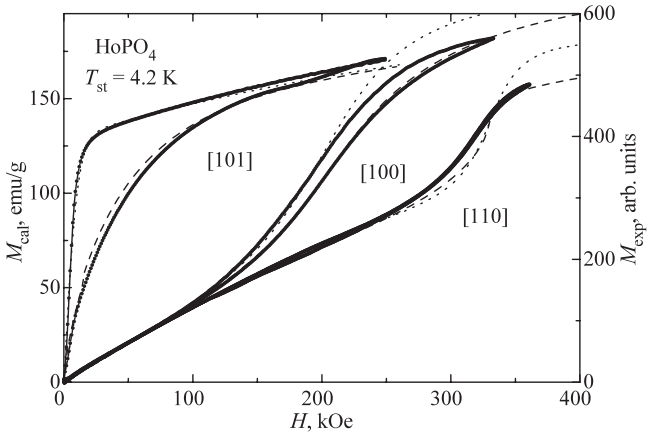


**Figure 1.** Experimental (points) and calculated adiabatic (dashed, $T_{st} = 4.2$ K) and isothermal (short dashed, $T_0 = 4.2$ K) curves of the magnetization for an $HoPO_4$ crystal in a magnetic field along the [101], [100] and [110] axes.

calculating the smoothed magnetization function $M(H)$ and its derivative $dM(H)/dH$. A related $DyPO_4$ crystal for which the magnetization along the easy axis [001] saturates sharply at $m_s = 10\ \mu_B$ was used to calibrate the absolute value of the magnetization. This calibration was found to be accurate to within ~30% because of the high sensitivity of the pick-up coil to the size and shape of a crystal. No correction for demagnetizing effect was made since for our samples the demagnetizing field did not exceed 3 kOe.

## 3. Experimental results

Experimental dependences of the magnetization $M(H)$ along the [101], [100], and [110] axes for an $HoPO_4$ crystal at $T_{st} = 4.2$ K are shown in figure 1. In a pulsed magnetic field one should distinguish a start temperature $T_{st}$ for the adiabatic regime and a temperature $T_0$ for the isothermal one which coincide only at $H = 0$. The arbitrary units are used for the experimental magnetization curves due to some uncertainty of the absolute value of the experimental data. For a magnetic field along the [101] direction between the easy [001] and hard [100] axes, the magnetization exhibits large hysteresis and does not reach the saturation value $m_s = 10\ \mu_B$ ($M_s = 214.9$ emu $g^{-1}$), corresponding to the total magnetic moment of the $Ho^{3+}$ ion. The magnetization along the [100] axis exhibits a smooth jump near the critical field $H_c \sim 200$ kOe, approaches ~8.5 $\mu_B$ above $H_c$, and continues to increase in higher fields. For $H \parallel [110]$, the value of the critical field increases to 320 kOe, the $M(H)$ curve varying more sharply near $H_c$. The critical field $H_c$ for both axes in the basal plane can be determined more accurately from the differential susceptibility curves $dM/dH$ (see section 5.3, figures 4, 5). As the temperature increases, the dependences $M(H)$ become more and more smeared and the critical field value changes slightly. The $M(H)$ and $dM(H)/dH$ curves exhibit a small hysteresis for the two axes in the basal plane. The higher the $dM(H)/dH$ value is, the larger the hysteresis. This gives evidence that the hysteresis originates mainly from the magnetocaloric effect in the increasing field.

## 4. Theoretical treatment

The complete Hamiltonian for a single 4f ion includes the Hamiltonian of the crystal field $H_{CF}$, the Zeeman, $H_Z$, and bilinear, $H_B$, terms, which describe the interaction of the 4f angular

momentum **J** with the external, **H**, and exchange, $\mathbf{H}_M$, fields, and the Hamiltonian of the quadrupolar interaction, $H_{\rm QT}$:

$$H = H_{\rm CF} + H_{\rm Z} + H_{\rm B} + H_{\rm QT}. \tag{1}$$

Using the equivalent operator method and the molecular field approximation for the pair bilinear and pair quadrupolar interactions, we can write these terms in the form (for details, see, for example, [14])

$$H_{\rm CF} = \alpha_J B_2^0 O_2^0 + \beta_J (B_4^0 O_4^0 + B_4^4 O_4^4) + \gamma_J (B_6^0 O_6^0 + B_6^4 O_6^4), \tag{2}$$

$$H_{\rm Z} = -g_J \mu_{\rm B} \mathbf{H} \cdot \mathbf{J}, \tag{3}$$

$$H_{\rm B} = -g_J \mu_{\rm B} \mathbf{H}_M \cdot \mathbf{J}, \qquad \mathbf{H}_M = n g_J \mu_{\rm B} \langle \mathbf{J} \rangle, \tag{4}$$

$$H_{\rm QT} = -G^\alpha \langle O_2^0 \rangle O_2^0 - G^\gamma \langle O_2^2 \rangle O_2^2 - G^\delta \langle P_{xy} \rangle P_{xy} \qquad (P_{xy} = \tfrac{1}{2}(J_x J_y + J_y J_x)). \tag{5}$$

Here $O_n^m$ and $\alpha_J$, $\beta_J$, $\gamma_J$ are the Stevens operator and the Stevens parameters, respectively; $B_n^m$ the crystal field parameters; $g_J$ and $\mu_{\rm B}$ the Lande factor and the Bohr magneton; and $n$ the bilinear exchange parameter. The $\gamma$ and $\delta$ modes in equation (5) correspond to the orthorhombic deformations of the tetragonal crystal structure along the [100] or [110] axes, respectively, and the $\alpha$ mode describes the tetragonal deformation, which appears either in an external magnetic field or in a quadrupolar ordered phase. The quadrupolar moments are determined by the eigenvalues $E_i$ and eigenfunctions $|i\rangle$ of the RE ion ($Z$ is the partition function)

$$\langle O_m^n \rangle = \alpha_J \sum_i \langle i | O_m^n | i \rangle \exp(-E_i / k_{\rm B} T)/Z \qquad (O_m^n = O_2^0, O_2^2, P_{xy}). \tag{6}$$

The total quadrupolar constants $G^\mu = G^\mu_{\rm ME} + K^\mu = (B^\mu)^2/C_0^\mu + K^\mu$ ($\mu = \alpha, \gamma, \delta$) include terms from both the one-ion magnetoelastic interaction, $B^\mu$, and the pair quadrupolar one, $K^\mu$ ($C_0^\mu$ is the background elastic constant in the absence of the interactions). In the Hamiltonian $H_{\rm QT}$, we omitted the $\varepsilon$-symmetry terms, which do not contribute for a magnetic field in the basal plane or along the tetragonal axis.

Parameters of the pair interactions for $HoPO_4$ were determined from the measurements of the first- and third-order magnetic susceptibilities and of the parastriction at low temperatures in relatively weak fields for all symmetry modes [15]. The magnetic interaction temperature $\theta_\parallel = n_\parallel C \approx -0.5$ K ($C = 2.52\ \mu_{\rm B}\ {\rm kOe}^{-1}$ is the Curie constant) was determined for the easy magnetization axis [001] from the magnetic susceptibility which gives rise, in accordance with experiment, to the Néel temperature $T_{\rm N} = 1.4$ K. It is not clear, however, whether the bilinear interactions are completely isotropic in the crystal. The quadrupolar constants $G^\mu$ in $HoPO_4$ do not lead to sizeable quadrupolar effects: for example, to the spontaneous quadrupolar ordering. However, their role is expected to increase in the vicinity of the crossover. In subsequent calculations, the maximal reasonable values for the bilinear and quadrupolar constants from [15] are used to estimate their effect: $\theta_\perp = -0.5$ K ($H \parallel [100]$, $H \parallel [110]$), $G^\alpha = 0.7$ mK, $G^\gamma = 1$ mK, and $G^\delta = 3$ mK.

The eigenvalues and eigenfunctions of the $Ho^{3+}$ ion, which are necessary for the calculations of thermodynamic properties, were determined by the numerical diagonalization of the complete Hamiltonian (1). The contributions of the bilinear interactions and of the quadrupolar interactions of $\alpha$ and $\gamma$ ($\delta$) symmetry, which depend themselves on the electron structure, were taken into account in a self-consistent way.

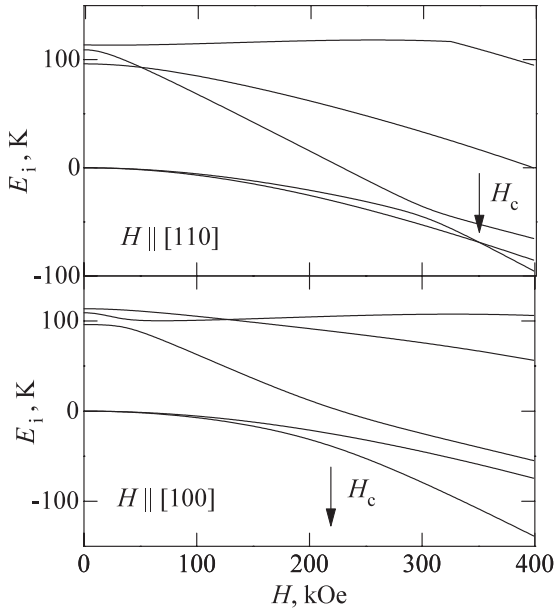


**Figure 2.** The energy variation of the lower levels of the $Ho^{3+}$ ion in $HoPO_4$ for a magnetic field along the [110] (top) and [100] (bottom) axes calculated without regard to the quadrupolar interactions.

## 5. Discussion of the results

### *5.1. Crystal field and Zeeman effect*

The CF parameters for $HoPO_4$ are believed to be reliably determined on the basis of numerous experimental data, including inelastic neutron scattering [16]. We used the CF parameters from [15] determined on the ground multiplet (in K): $B_2^0 = 265$, $B_4^0 = 4$, $B_4^4 = 956$, $B_6^0 = -60$, $B_6^4 = 54$. The $Ho^{3+}$ ion spectra calculated with these parameters in the magnetic field oriented along the [100] and [110] axes (the Zeeman effect) are presented in figure 2. The figure shows only the five lower levels, which make the major contribution to the magnetic properties at low temperatures. The overall ground multiplet splitting coming up to 430 K at $H = 0$ does not shown in the figure. The energy of the doublet ground state at $H = 0$ is taken as the origin. In the phosphate structure, the ground multiplet ${}^5I_8$ of the $Ho^{3+}$ ion is split in such a way that the ground state is an 'isolated' doublet with a large $z$ component of the $g$-tensor and a small $x$ component. The next three excited singlets are separated by a gap of about 100 K and have a large component of the $g$-tensor in the basal plane ($g_\perp^{ex,i} \gg g_\parallel^{ex,i}$, $i = 1, 2, 3$). In the $J$, $J_z$ representation, the wavefunction of the lowest doublet is $0.99|\pm 7\rangle$; for the two excited singlets, it is $\{0.62|6\rangle - 0.35|2\rangle + 0.35|-2\rangle - 0.62|-6\rangle\}$ and $\{-0.24|4\rangle + 0.94|0\rangle - 0.24|-4\rangle\}$, respectively. These specific features of the spectrum and wavefunctions of the $Ho^{3+}$ ion determine its Ising properties and are favourable for an energy level crossing at a magnetic field oriented in the basal plane.

As expected, the ground doublet is weakly split in both $H \parallel [100]$ and $H \parallel [110]$ below the critical field, $H_c$, whereas the energy of the first or second excited singlets decreases strongly. As a result, the first (for $H \parallel [100]$) or second (for $H \parallel [110]$) excited singlet with the large component $\langle M_\perp \rangle$ ($M_{100}$, $M_{110}$) of the magnetic moment approaches, at a critical field $H_c$, the ground doublet with the small component $\langle M_\perp \rangle$, causing an increase of the magnetic moment.

The magnetic fields $H \parallel [100]$ and $H \parallel [110]$ strongly mix the wavefunctions of the singlets and the lower or upper component of the split doublet, which results in a repulsion of the interacting levels. For the case of $H \parallel [110]$ a quite unusual situation takes place when the upper component of the ground doublet crosses its lower one.

A characteristic feature of the Zeeman effect for $H \parallel [100]$ is the presence of a large gap of about 40 K between the interacting levels, i.e. the low component of the ground doublet and the first exited singlet, at the critical field $H_c = 210$ kOe since the field mixes the wavefunctions of the levels. In contrast, for the field along the [110] axis, there is no gap between the lowest levels at the crossover within the frame of the Hamiltonian used. A gap appears only at a small deviation of the field from the symmetry axis. Due to the finite gap at the crossover for $H \parallel [100]$, smoother dependences of the magnetic properties on the temperature and magnetic field are expected. For this case a misorientation of the field from the symmetry axis both in and out of the basal plane is less important than for the crossover without a gap.

The calculation with the inclusion of only the crystal field and Zeeman terms yields values of the critical field ∼210 and 350 kOe for $H \parallel [100]$ and $H \parallel [110]$, respectively, corresponding to the closest approach or crossing of the lower levels and to the maximum in the differential susceptibility curve $\mathrm{d}M/\mathrm{d}H$. These values are higher than the experimental ones for both field orientations. Note that the demagnetization field for our sample does not exceed 3 kOe, and increases still further the value of $H_c$. Since the CF parameters for $HoPO_4$ are determined quite reliably, this discrepancy can be considered as indicative of an additional contribution from the pair, mainly the quadrupolar interactions. The quadrupolar interactions become more important in fields higher than $H_c$, and cause a sizeable change of the magnetic properties. A similar decrease of the critical field, $H_c$, was observed for $DyPO_4$ [15] and was found to be caused by quadrupolar interactions.

### *5.2. Magnetization curves and magnetocaloric effect*

In order to interpret the magnetic properties in pulsed fields with sufficiently small pulse duration, one must take into account the magnetocaloric effect. We assume that the magnetization process of the $HoPO_4$ crystal in our experiment is close to the adiabatic and isothermal ones for increasing and decreasing fields respectively. The subsequent comparison of the calculations with the experimental data confirms this assumption.

When calculating the magnetic properties, the complete Hamiltonian was numerically diagonalized for every field value from 0 to 400 kOe in steps of $\Delta H = 1$ kOe in order to determine the electron structure of the $Ho^{3+}$ ion, and the 'elementary' magnetocaloric effect $\Delta T$ was calculated for the field change from $H$ to $H + \Delta H$:

$$\Delta T = -(\partial M/\partial T)_H T \Delta H / C_H. \tag{7}$$

In formula (7), the total heat capacity of the crystal, $C_H$, includes the lattice heat capacity $C_{\mathrm{lat}} = (12\pi^4 k_B \nu/5)(T/T_D)^3$ (the Debye temperature for the phosphate lattice is $T_D = 275$ K [17] and the number of atoms per formula $\nu = 6$) and the magnetic heat capacity, $C_{\mathrm{mag}}$, calculated for every value of the field and temperature on the basis of the RE ion spectrum. These data make it possible to calculate the sample temperature and adiabatic magnetization of the $HoPO_4$ crystal. The isothermal and adiabatic magnetization curves along the three symmetry axes [001], [100], and [110] calculated with regard to the quadrupolar interactions and the corresponding curves of the magnetocaloric effect $\Delta T$ for the initial temperatures $T_{\mathrm{st}} = 4.2$ and 20 K are shown in figure 3.

For a magnetic field along the easy axis [001], the magnetization rises sharply to the constant value 8.7 $\mu_B$, which is less than the total magnetic moment 10 $\mu_B$ of the free $Ho^{3+}$

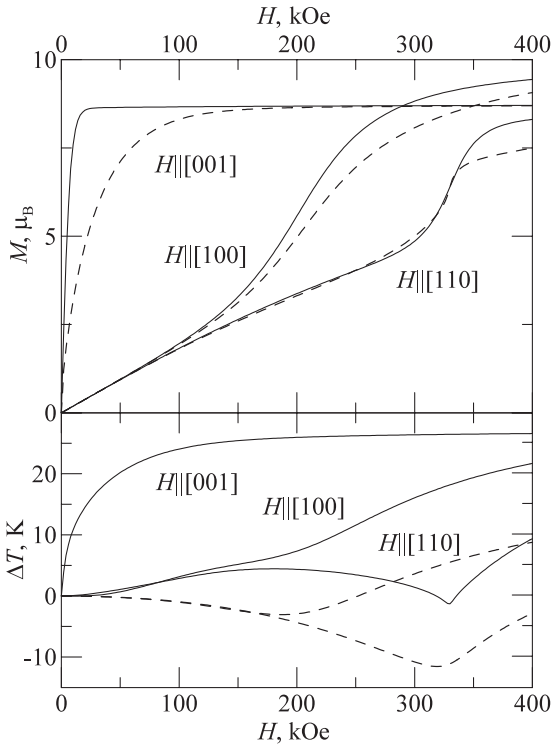


**Figure 3.** Isothermal (solid curves, $T_0 = 4.2$ K) and adiabatic (dashed curves, $T_{st} = 4.2$ K) magnetization curves $M(H)$ (top) and magnetocaloric effect $\Delta T$ (bottom; solid curves at $T_{st} = 4.2$ K and dashed curves at $T_{st} = 20$ K) for $HoPO_4$ in a magnetic field along the [001], [100] and [110] axes calculated with regard to the quadrupolar interactions.

ion. This value corresponds to the full contribution from the lowest doublet $|\pm 7\rangle$. The total saturation is expected to take place by a jump at $H_c \sim 300$ T since the level with the large component $|\pm 8\rangle$ lies high enough and is not mixed with the lowest doublet by the field $H \parallel [001]$. The calculated magnetization curves in the basal plane describe the main features of the experimental ones. The closeness of the lower energy levels gives rise to the smeared magnetization jump in the field along the [100] axis, while the energy level crossing for $H \parallel [110]$ results in the sharper jump in the isothermal curves. The magnetic moment after the crossover does not reach the saturation value for both symmetry axes in the basal plane. The magnetization along the [100] axis increases by a smooth jump from $\sim 2\ \mu_B$ up to $\sim 7\ \mu_B$ at the critical field $H_c \sim 200$ kOe. For $H \parallel [110]$, the critical field $H_c \sim 320$ kOe is higher and the jump is smaller. Note that the critical field values are very close to the experimental ones when taking into account the quadrupolar interactions.

For $H \parallel [100]$, the magnetization jumps in the isothermal regime vary weakly with temperature. This explains why the magnetization is slightly smeared for the adiabatic process, at the end of which the temperature increases by 20 K. Due to the finite gap in the spectrum, the jump in the $M(H)$ curves for the field along the [100] axis remains more smeared than that for the [110] axis at $T = 4.2$ K and especially at $T = 1.4$ K. In the case of the crossover without a gap for $H \parallel [110]$, the magnetization jump and susceptibility maximum become infinitely sharp at $T \to 0$ within the frame of the Hamiltonian used.

In the adiabatic regime, the magnetization changes more slowly along the [001] and [100] axes and, in contrast, more sharply along the [110] axis, due to an anisotropic magnetocaloric effect in the $HoPO_4$ crystal. Thus in the adiabatic curves the difference between the magnetic anomalies for the two axes in the basal plane becomes more noticeable. The maximal magnetocaloric effect $\Delta T \sim 25$ K is observed in the field along the easy axis [001]. For both axes in the basal plane, the variation of the sample temperature is small in fields weaker than the crossover field ($\Delta T < 10$ K), since the magnetization changes weakly. In fields near and above $H_c$, the sample heats noticeably for $H \parallel [100]$ and cools down for $H \parallel [110]$. For $H \parallel [100]$, the sample temperature varies monotonically with field for the starting temperature $T_{st} = 4.2$ K; however, the rate of the temperature variation decreases near $H_c$. For higher starting temperatures $T_{st} = 20$ K, the magnetocaloric effect becomes non-monotonic for both field orientations in the basal plane, and it is accompanied by cooling of the sample near $H_c$ (see the dashed curves in figure 3). This is related to a complex behaviour of the derivative $(\partial M/\partial T)_H$ with temperature near the crossover.

The calculated magnetization curves are compared with the experimental ones in figure 1. Two different axes are used for calculated and experimental curves due to some uncertainty of the absolute value of the experimental data, the scales for these axes being dovetailed on the basis of the magnetization in low fields [15]. It is seen that the experimental data for increasing fields are described quite well by the adiabatic curves while those for decreasing fields are described better by the isothermal curves except for the transition range just after the change of the sign of the derivative $\mathrm{d}H/\mathrm{d}t$. The larger pulse duration for decreasing field ($\sim$700 ms) is believed to be the main reason for the change of the magnetization processes to the isothermal one. The difference between the adiabatic and isothermal curves as well as the difference between the magnetization for increasing and decreasing fields are more pronounced for a magnetic field orientation close to the easy axis (axis [101] in figure 1) where the magnetocaloric effect is larger. The discrepancy for the [110] axis may be explained by a small field misorientation which strongly affects the critical field value and susceptibility peak (see below).

### *5.3. Differential magnetic susceptibility*

The experimental data and theoretical analysis show that the behaviour of the $M(H)$ curves is sensitive to quadrupolar interactions. This dependence can be conveniently analysed by using differential curves $\mathrm{d}M/\mathrm{d}H$. Figures 4 and 5 display the experimental and calculated adiabatic and isothermal derivatives $\mathrm{d}M/\mathrm{d}H$ for $H \parallel [100]$ at $T = 4.2$ K and for $H \parallel [110]$ at $T = 1.4$ and 4.2 K, respectively. For $H \parallel [100]$, the comparison of the adiabatic curves at $T_{st} = 4.2$ K calculated with regard (solid curve 2) and without regard (dashed curve 4) to the quadrupolar interactions shows that these interactions reduce the critical field and move it closer to the experimental value. In the process, the maximum of the $\mathrm{d}M/\mathrm{d}H$ curve increases, and its width decreases. To separate the contributions from the different terms in $H_{QT}$ (equation (5)), the $M(H)$ and $\mathrm{d}M(H)/\mathrm{d}H$ curves were calculated successively with the inclusion of the bilinear, $\alpha$ and $\gamma$ low-symmetry quadrupolar interactions. The negative bilinear interactions with $\theta_\perp = -0.5$ K increase $H_c$ by only $\sim$2 kOe. In contrast, the inclusion of quadrupolar interactions with $G^\alpha = 0.7$ mK and $G^\gamma = 1$ mK reduces the critical field down to $\sim$200 kOe, while the peak in the $\mathrm{d}M/\mathrm{d}H$ curve becomes stronger and narrower, in accordance with the experiment. The main contribution comes from the totally symmetric quadrupolar constant $G^\alpha = 0.7$ mK; the low-symmetric one $G^\gamma = 1$ mK only slightly modifies the data. Note that for $HoPO_4$ the effect of quadrupolar interactions is smaller than for $DyPO_4$ [8], but it moves the calculated curves $M(H)$ and $\mathrm{d}M(H)/\mathrm{d}H$ very close to the experimental ones.

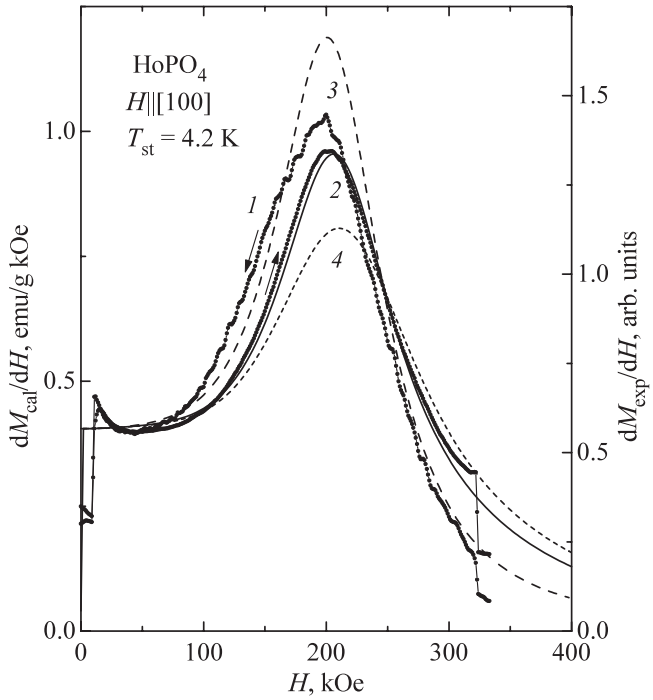


**Figure 4.** The experimental (points, curve 1) and theoretical susceptibility $dM/dH$ of $HoPO_4$ at the field orientation $H \parallel [100]$ and $T_{st} = 4.2$ K calculated in adiabatic or isothermal (curve 3) regimes with regard (curves 2, 3, $G^{\alpha} = 0.7$ mK, $G^{\gamma} = 1$ mK) and without regard (curve 4) to quadrupolar interactions.

Similar regularities are observed for $H \parallel [110]$, where the effect of quadrupolar interactions is larger in value (see figure 5). The peak in the $dM/dH$ curves calculated without the quadrupolar interactions (curves 3 and 2 in the figure and inset, respectively) is large and narrow but the critical field of the crossover is noticeably higher. As is seen from the inset, a small misorientation of the magnetic field $\sim$1–2° out of the symmetry axes both in ($\Delta\varphi_{\perp}$, curve 4) and out of ($\Delta\varphi_{\parallel}$, curve 3) the basal plane results in the smoothing of the magnetic anomalies. Then the critical field increases for $\Delta\varphi_{\parallel}$ but decreases for $\Delta\varphi_{\perp}$, the change being $\Delta H_c \sim 10$ kOe for $\Delta\varphi_{\perp} = 2°$. It is impossible, however, to achieve the experimental values of the critical field, $H_c$, and the width of $dM/dH$ by changing only the value of $\Delta\varphi_{\parallel}$ or $\Delta\varphi_{\perp}$. Quadrupolar interactions decrease the critical field, and the maximum of the $dM/dH$ curves becomes greater and narrower (curve 2 in figure 5), which is in better agreement with the experiment. The experimental data are described quite well with the same quadrupolar constant $G^{\alpha} = 0.7$ mK and $G^{\delta} = 3$ mK when taking into account a small possible misorientation $\Delta\varphi_{\perp} \sim$ 1–2° in the basal plane (curve 2′), where again the main contribution comes from the $G^{\alpha}$ constant.

For crossover without a gap at $H \parallel [110]$, an interesting problem of magnetic ordering arises. A high magnetic field in the basal plane destroys the antiferromagnetic ordering which appears along the tetragonal axis below 1.4 K. A small peak in the $dM/dH$ curve at $H \parallel [110]$ which appears near 150 kOe only below $T_N = 1.4$ K (curve 1 in figure 5) probably originates from the destruction of the magnetic order. Our calculations with the above-mentioned magnetic interaction temperatures $\theta_{\parallel} = -0.5$ K give rise to the critical field of the spin-flip transition $H_{sf} \sim 150$ kOe for $H \parallel [110]$. We emphasize that the degenerate

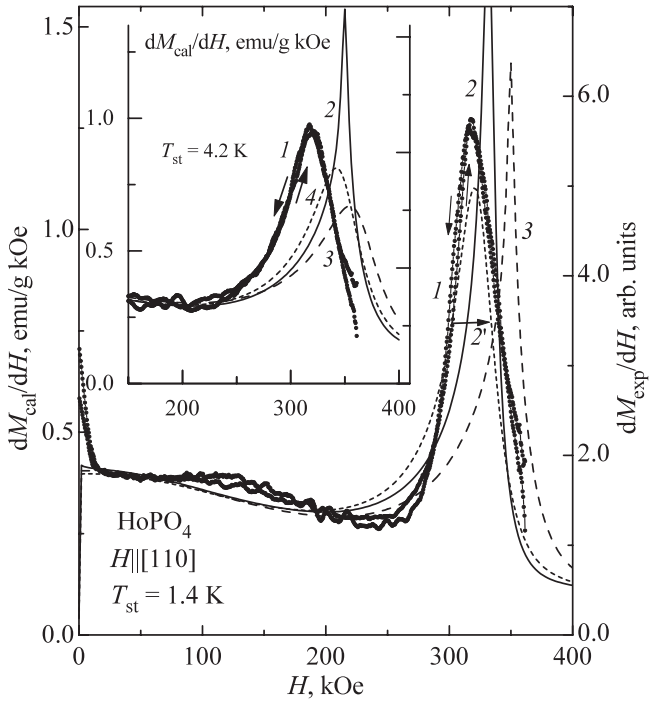


**Figure 5.** The experimental (points, curve 1) and theoretical susceptibility $dM/dH$ of $HoPO_4$ at the field orientation $H \parallel [110]$ and $T_{st} = 1.4$ K calculated with regard ($G^{\alpha} = 0.7$ mK, $G^{\delta} = 3$ mK; curve 2—$\Delta\varphi_{\parallel} = \Delta\varphi_{\perp} = 0$, 2′—$\Delta\varphi_{\perp} = 1.5°$) and without regard (curve 3—$\Delta\varphi_{\parallel} = \Delta\varphi_{\perp} = 0$) to the quadrupolar interactions. The inset shows experimental (points, curve 1) and theoretical susceptibility $dM/dH$ of $HoPO_4$ and $T_{st} = 4.2$ K calculated without regard to the quadrupolar interactions for various misorientations from the symmetry axis (curve 2—$\Delta\varphi_{\parallel} = \Delta\varphi_{\perp} = 0$, 3—$\Delta\varphi_{\parallel} = 2°$, 4—$\Delta\varphi_{\perp} = 2°$).

ground state near $H_c$ is known to be unstable and sensitive to small pair interactions which may remove the degeneracy. For example, the weak bilinear interaction may give rise to the appearance of the perpendicular (relative to a magnetic field) component of the magnetic moment near $H_c$ at low temperature, i.e. along the [001] axis or second equivalent [110] axis. Additional investigations below 1 K are necessary to ascertain the possibility of this transition.

The differential curves also make it possible to compare the experimental data with the calculated ones in the adiabatic and isothermal regimes (curves 2, 3 in figure 4) accurately. The calculated adiabatic curve $dM/dH$ for $H \parallel [100]$ describes the experimental data for increasing field rather well. For the isothermal $dM/dH$ curve, the maximum is slightly shifted to lower fields, which is in better agreement with the experimental data for decreasing fields. The main difference between the isothermal and adiabatic curves $dM/dH$ is in their shape. In the adiabatic mode, the curve is asymmetric and is more extended for $H > H_c$; this is due to the heating of the sample in fields higher than the critical one. The isothermal curve is almost symmetric, i.e., the location of the peak centre is the same at any height. The comparison shows that the experimental curve is as asymmetric as the adiabatic $dM/dH$ curve for increasing field, and more symmetric for decreasing field. Thus, the experiment testifies that the magnetization process of paramagnets is close to the adiabatic one in pulsed fields of 100 ms duration. For pulsed fields of 700 ms duration, the experimental data are described better by the isothermal curves.

We stress that all calculations were performed without any adjustable parameters and were based only on the interaction parameters determined from independent experiments in relatively small fields. When the calculations are performed with the known quadrupolar constants, both the critical field, $H_c$, and the peak in the $dM/dH$ curve are very close to the experimental ones for two axes in the basal plane. The values of the constants $G^\mu$ were determined on the basis of the magnetoelastic coefficients $B^\mu$ found by measuring the parastriction and the elastic constants $C^\mu$ averaged over the RE phosphate series. In the process, only the contribution to $G^\mu$ from the one-ion magnetoelastic interaction was taken into account, since no reliable data on the parameters of the pair quadrupolar interaction (which usually yields a considerably smaller contribution in RE zircons) are available. Taking into account this fact, we find that the agreement with the experimental data is quite good.

### *5.4. The effect of quadrupolar interactions*

The quadrupolar interactions modify the $Ho^{3+}$ ion spectrum near the crossover and thus alter various thermodynamic characteristics, in particular, the magnetization and magnetic susceptibility curves. A sharp increase in the quadrupolar contributions is caused by a change of the quadrupolar moments of the $Ho^{3+}$ ion at $H > H_c$. The quadrupolar moments at $T = 1.4$ K calculated with and without the quadrupolar interactions for a magnetic field along the two axes in the basal plane are shown in figure 6. Because of a strong modification of the $Ho^{3+}$ electronic structure, the quadrupolar moment $\langle O_0^2 \rangle$ decreases near the crossover, and a large quadrupolar moment $\langle O_2^2 \rangle \approx 50$ for $H \parallel [100]$ or $\langle P_{xy} \rangle \approx 13$ for $H \parallel [110]$ simultaneously arises. This signifies that the contributions from both terms in the $H_{QT}$ Hamiltonian (see equation (5)) noticeably change.

A change of the contribution from the quadrupolar interactions of $\alpha$ symmetry $-G^\alpha \Delta Q_0 O_2^0$ ($\Delta Q_0 = \langle O_2^0 \rangle(H) - \langle O_2^0 \rangle(0) < 0$) in a magnetic field reduces the effective second-order CF parameter $B_2^0$ and diminishes the critical field. The contribution to the second-order CF parameter $\Delta B_2^0 = -G^\alpha \langle O_2^0 \rangle / \alpha_J$ takes also place without a magnetic field and varies with temperature due to the change of the quadrupolar moment $\langle O_2^0 \rangle$. This addition differs across the RE phosphate series, and for the Ho ion amounts to ~10% of the zero-field parameter at 4.2 K. The calculations with and without $-G^\alpha \langle O_2^0 \rangle / \alpha_J$ give rise to the energy of the first excited singlets differing by ~1–6 K. Similarly, the $\gamma(\delta)$ quadrupolar interactions $-G^\gamma \langle O_2^2 \rangle (-G^\delta \langle P_{xy} \rangle)$, though being negligible in the absence of a magnetic field, diminish the critical field after the $\langle O_2^2 \rangle$ ($\langle P_{xy} \rangle$) moment increases jumpwise near the crossover. Thus, both types of interaction noticeably decrease the critical field, the strongest effect being for the case of $H \parallel [110]$.

The crossover in $HoPO_4$ is accompanied by variations of various quadrupolar moments of the $Ho^{3+}$ ion at low temperatures, which cause anomalies of various components of the magnetostriction deformation. The investigation of the magnetostriction anomalies under crossover is rather informative, since it makes it possible to determine or refine the values of the magnetoelastic coefficients in addition to determining the critical field $H_c$. Besides, the magnetostriction anomalies, which are directly related to the variation of the quadrupolar moments, enable one to estimate the role of quadrupolar interactions in the effects studied.

## 6. Conclusions

In conclusion, we formulate the main results obtained in this study. The crossover in the $HoPO_4$ crystal is accompanied by a jump of the magnetic moment of the $Ho^{3+}$ ion as well as of the quadrupolar ones at low temperatures. A specific feature of $HoPO_4$ is that for two

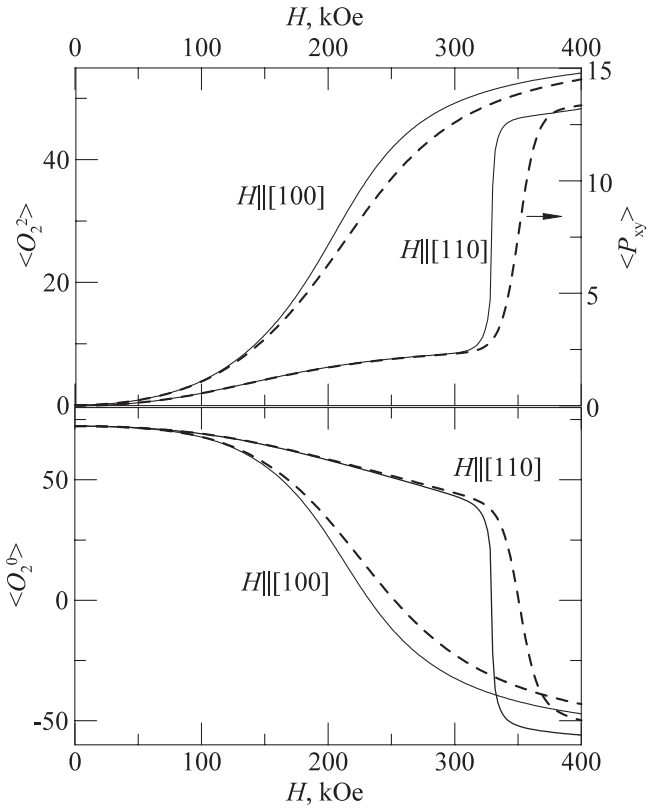


**Figure 6.** The isothermal quadrupolar moments $\langle O_2^0 \rangle$ (bottom) and $\langle O_2^2 \rangle$, $\langle P_{xy} \rangle$ (top) of $HoPO_4$ at a field orientation along the [100] and [110] axes and $T_0 = 1.4$ K calculated with regard (solid curves) and without regard (dashed curves) to the quadrupolar interactions.

symmetry axes in the basal plane a different type of crossover (with and without energy gap) takes place, resulting in magnetic anomalies of different character. For $H \parallel [100]$, there exists a finite gap of about 40 K between the approaching levels at the crossover. Due to this fact, the anomalies in the magnetization curves remain rather smeared down to very low temperatures. In contrast, a true crossing without a gap takes place for $H \parallel [110]$, resulting in much sharper magnetic anomalies at the critical field, which is however more sensitive to a misorientation.

A considerable advantage of the system studied is that it is relatively simple, and there is reliable information on the interaction parameters. This enables us to compare theoretical and experimental data quantitatively. In particular, this comparison shows that under pulsed fields of 100 ms duration the magnetization process is close to the adiabatic one and is accompanied by a considerable magnetocaloric effect.

The magnetic field is found to modify the electronic structure of the $Ho^{3+}$ ion in such a way that the quadrupolar effects near and above the crossover field, $H_c$, become more important. A considerable change in the quadrupolar moments at the crossover results in an increase of the contribution from the quadrupolar terms of the $\alpha$ and $\gamma(\delta)$ symmetry for $H \parallel [100]$ and $H \parallel [110]$, respectively, in the quadrupolar Hamiltonian $H_{QT}$. Note that under crossover the quadrupolar moment $\langle O_2^2 \rangle (\langle P_{xy} \rangle)$ increases jumpwise at the critical field $H_c$, which is characteristic of a stimulated quadrupolar transition.

These studies leave open some interesting questions. According to the calculations, the Zeeman effect for lower levels in the presence of quadrupolar interactions is of a more complex character, and depends on the constants of the quadrupolar interactions. In this context, experimental studies of the Zeeman effect near the crossover for RE zircons, in particular, for $HoPO_4$, are of evident interest. Besides, the experimental search for an induced magnetic transition near $H_c$ at $H \parallel [110]$ due to weak bilinear interactions may be interesting below 1 K.

## Acknowledgments

This work was partially supported by the Russian Foundation for Basic Research (project no 03-02-16809) and the International Science and Technology Centre (project no 2029).

## References

[1] Kazei Z A, Kolmakova N P, Platonov V V, Shishkina O A and Tatsenko O A 1997 *3rd Int. Conf. on f-Elements (Paris, 1997)* (Abstracts)
[2] Battison J E, Kasten A, Leask M J M and Lowry J B 1977 *J. Phys. C: Solid State Phys.* **10** 323
[3] Goto T, Tamaki A, Fujimura T and Unoki H 1986 *J. Phys. Soc. Japan* **55** 1613
[4] Morin P, Rouchy J and Kazei Z 1995 *Phys. Rev.* B **51** 15103
[5] Kazei Z A, Kolmakova N P, Levitin R Z, Platonov V V, Sidorenko A A and Tatsenko O M 1998 *Physica* B **246/247** 483
[6] Kazei Z A, Kolmakova N P, Platonov V V, Sidorenko A A and Tatsenko O M 2000 *Physica* B **284–288** 1483
[7] Kirste A, Puhlmann N, Stolpe I, Mueller H-U, von Ortenberg M, Tatsenko O M, Platonov V V, Kazei Z A, Kolmakova N P and Sidorenko A A 2001 *Physica* B **294/295** 132
[8] Kazei Z A and Snegirev V V 2001 *JETP Lett.* **73** 90
[9] Gehring G A and Gehring K A 1975 *Rep. Prog. Phys.* **38** 1
[10] Morin P and Kazei Z 1997 *Phys. Rev.* B **55** 8887
[11] Cooke A H, Swithenby S J and Wells M R 1973 *J. Phys. C: Solid State Phys.* **6** 2209
[12] Laugsch J, Kahle H G, Schwab M and Wuchner W 1975 *Physica* B **80** 269
[13] Neogy D, Sen H and Wanklyn B M 1989 *J. Magn. Magn. Mater.* **78** 387
[14] Morin P, Rouchy J and Schmitt D 1988 *Phys. Rev.* B **37** 5401
[15] Morin P and Kazei Z 1999 *J. Phys.: Condens. Matter* **11** 1289
[16] Loong C-K, Soderholm L, Hammonds J P, Abraham M M, Boatner L A and Edelstein N M 1993 *J. Phys.: Condens. Matter* **5** 5121
[17] Kasten A, Kahle H G, Klofer P and Schafer-Siebert D 1987 *Phys. Status Solidi* b **144** 423